

YANKEE ATOMIC ELECTRIC COMPANY

Telephone (508) 779-6711
TWX 710-380-7619



580 Main Street, Bolton, Massachusetts 01740-1398

December 12, 1989
BYR 89-175

United States Nuclear Regulatory Commission
Document Control Desk
Washington, DC 20555

Attention: Mr. Robert C. Jones, Acting Chief
Reactor Systems Branch
Division of Engineering and Systems Technology
Office of Nuclear Reactor Regulation

References: (a) License No. DPR-3 (Docket No. 50-29)
(b) USNRC Letter to YAEC, "Request for Additional Information
for Topical Report YAEC-1363," dated November 13, 1989

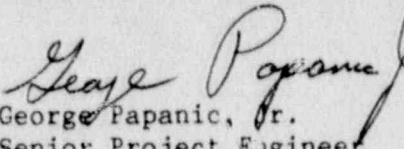
Subject: Additional Information on YAEC-1363, "CASMO-3G Validation"

Dear Mr. Jones:

Reference (b) requested additional information in support of the subject topical report. Enclosed are the responses to your questions. We trust that you will find this information satisfactory. However, should you desire further information or clarification, please contact Mr. Richard Cacciapouti of our staff.

Very truly yours,

YANKEE ATOMIC ELECTRIC COMPANY


George Papanic, Jr.
Senior Project Engineer
Licensing

GP/gjt/0672v

Attachments

cc: USNRC Region I
USNRC Resident Inspector, YNPS

Aoo'
1/1

RESPONSES TO REQUEST FOR ADDITIONAL INFORMATION
CONCERNING YAEC-1363, CASMO-3G VALIDATION
QUESTIONS AND ANSWERS

- 1) Q. *What error is introduced in the gamma detector response/bundle power correlation by using the 10 group rather than the 18 group library?*
- A. The energy group structures for the 10 group and 18 group libraries are provided in Table 1.3 of YAEC-1363. The 10 group library maintains essentially the same energy group definition as the 18 group library for the lower energy groups up to 1.0 MeV, with a coarser energy group structure in the high energy range. The gamma energy distribution in a Westinghouse 3.1 w/o unshimmed assembly is provided in Figure 1.1 for both the 18 group and 10 group gamma cross section libraries. Comparison of these energy spectra demonstrates that the loss in clarity at the high energy levels with the 10 group library results in a small effect on the overall gamma flux energy and spatial distribution. The total detector responses were calculated for this problem using the CASMO-3G default gamma detector sensitivity functions for iron, and were 2.030×10^{23} 1/cc-sec and 2.033×10^{23} 1/cc-sec for the 18 group and 10 group libraries, respectively. This represents a detector response difference of 0.15 percent.
- 2) Q. *What specific effect required the addition of a new energy group (group 32) to the 69 group neutron library?*
- A. Energy group 32 was added to the 69 group neutron library in order to provide a 1.855 eV boundary for editing purposes. Addition of this group has an insignificant effect on the calculation process.
- 3) Q. *Describe the adjustments to the U-238 and silver/indium resonances made to improve agreement with measurement data.*
- A. Most of the cross section data was obtained from ENDF/B-IV, with some fission spectra data from ENDF/B-V. The U-238 resonances are adjusted to agree with Hellstrand's resonance integral measurements. Earlier versions of CASMO-3G had minor adjustments in the strongly shielded silver and indium resonances for control rods. However, for the latest version of CASMO-3G, resonance self shielding in silver and indium is calculated with no adjustments to the silver and indium resonance library data.
- 4) Q. *Describe the "special" transport calculation for the fuel, clad, and*

moderator regions which is used to describe the unit-cell buffer region.

- A. The "special" transport calculation in MICBURN-3, mentioned in page 10 of YAEC-136², refers to the homogenization process used to calculate buffer zone cross sections for use in the main transport calculation of the absorber pin, clad, moderator, and buffer zone. The calculation is made using collision probabilities in the three regions (fuel, clad, and moderator) which define the uniform lattice of the buffer zone. The flux distribution obtained from this calculation is used to calculate cross sections for the homogenized buffer zone. The word "special" was used to differentiate the buffer zone calculation from the main transport calculation.

5) Q. Describe the procedure used to treat the BWR control rod wing which preserve the rod blackness.

- A. Effective cross sections for a cruciform control rod which contains cylindrical absorbers are determined such that the region averaged reaction rates and fluxes are preserved in the 2D COXY calculation, where the control rod is represented as a homogeneous slab. This process consists of the resonance calculation, microgroup calculation, macrogroup calculation, and cross section homogenization using control rod collision probabilities. These steps are described in detail below.

RESONANCE CALCULATION: The 40 or 70 group cross section library is adjusted for resonance absorbers via a collision probability calculation similar to that performed for a cluster control rod. Dancoff factors are calculated using the same method as for fuelled cells with the fuel cell pitch replaced by the pitch between the absorber cylinders, and with the moderator replaced by the cruciform rod structural material. An effective Dancoff factor is used which properly accounts for the cylindrical absorbers at the end of the cruciform blade.

MICROGROUP CALCULATION: The microgroup calculation is performed to obtain detailed neutron energy spectra to be used for energy condensation and spatial homogenization of the individual poison rods. This is performed with a homogenized buffer region surrounding the poison rod/cladding/coolant cell. The buffer region is defined by a microgroup calculation consisting of a lattice averaged fuel rod, cladding, and moderator regions. The buffer region is 2.5 mean free paths (at .625 eV for the 70 group library or .500 eV for the 40 group library) in radial thickness.

Flux spectrum correction factors are calculated for the poison rod which properly account for the differences in the calculated spectra between a homogenized absorber cell and one explicitly modelled. These factors are condensed to the 2D group structure for use in the

COXY calculation, along with the flux-volume homogenized cross sections, in order to preserve the reactivity and reaction rates in the lattice.

MACROGROUP CALCULATION: The macrogroup calculation is performed in cylindrical geometry with the cross sections for the regions determined by flux and volume weighting of the pin cells from the microgroup calculation. The calculation is performed twice, once for the geometry with the wide water gap as the outermost annulus and once for the same geometry with the narrow water gap. The resulting fluxes are used to collapse the lattice cross sections to the 2D calculation energy group structure. The flux energy spectra from this calculation are used for the homogenization of the control rod cross sections.

HOMOGENIZED CROSS SECTIONS: Cross sections for the 2D COXY calculation are calculated using a Control Rod Collision Probability subroutine, CROCOP. The microgroup cross sections are collapsed into macrogroup cross sections by flux weighting using the moderator spectrum from the pin cell calculation. Condensation to the 2D group structure is accomplished via flux weighting with the control rod flux obtained from the macrogroup calculation.

The neutron current into the homogenized control blade is calculated in the macrogroup structure using escape probabilities. The neutron current is collapsed to the 2D group structure and then used to calculate the flux distribution within the blade. The geometrical model used to calculate the flux distribution is an infinite array of absorber cells, with each cell divided into two regions. The inner region contains the absorber material and the surrounding rectangular region contains the structural material and moderator. Effective cross sections are then determined such that the blackness is preserved for each energy group in the 2D calculation group structure.

- 6) Q. *Discuss in detail the applicability of the COXY neutron transport collision probability code to the calculation of gamma transport. For example, what is the effect of the "nearest neighbor" coupling assumption in the gamma transport calculations?*
- A. CASMO-3G uses the transmission probability routine COXY for the gamma transport calculation. This model is equally applicable to gamma transport problems as it is to neutron transport. Although the numeric solution to the transport problem is solved with coupling only between neighboring meshes, the gamma (or neutron) transport from any individual mesh to another mesh anywhere in the bundle is accurately modeled by the transmission probabilities and interface currents on mesh surfaces.

An older CASMO version, CASMO-1G, used the collision probability

module CPM for the gamma transport calculation. The CPM approach is accurate but very slow. The more efficient COXY model was therefore chosen for CASMO-3G.

To illustrate the validity of the COXY module, gamma detector responses were calculated using CASMO-3G and CASMO-1G at 0%, 40%, and 70% void for exposures from 0 to 20 GWd/T for Bundle Type 5 in the Hatch BWR, as reported in Section 2.6 of YAEC-1363. The two models agreed closely, with an RMS difference of 1.16 percent and a maximum difference of 2.73 percent.

7) Q. *Is the gamma transport theory option applicable to PWR assemblies?*

A. Yes. Results using this option are presented as part of the answer to Question 1. The option is used to calculate Seabrook Station's fixed gamma detector power to signal response functions.

8) Q. *How large are the G-factor material dependent multipliers for typical BWR and PWR assemblies?*

A. G-factors are used as multipliers on the absorption cross section in areas of strong gradients to match fine mesh diffusion solution (DIXY) reaction rates to the more accurate transport solution (COXY). This improves the accuracy of fine mesh diffusion theory codes such as PDQ. However, the new methods described in YAEC-1363 and in YAEC-1659 do not involve the use of a fine mesh diffusion theory code such as PDQ, so G-factors are not used.

Nevertheless, G-factors for unshimmed and 8 shim 14 x 14 CE PWR lattices were provided in Table 2.4 of YAEC-1363 and are presented in Table 8.1 with the relative absorption rate differences presented for the individual regions of the assembly (Table 2.4 provided the maximum relative difference).

G-factors for a Vermont Yankee 8 x 8 CE BWR high energy bundle at 40% void are presented in Table 8.2. This bundle contains seven fuel rods of three different U-235 enrichments which contain 5 w/o gadolinia burnable absorber. There are also four water rods, and the wide and narrow water gap regions. G-factors are calculated for each of these regions and are presented in Table 8.2 along with the relative absorption rate differences between the DIXY and COXY calculations, with and without use of the G-factors.

Tables 8.1 and 8.2 demonstrate the difficulty that diffusion theory has in modeling strongly heterogeneous lattices without using G-factors. The CASMO-3G / SIMULATE-3P methodology utilizes the COXY calculated intra-assembly detail when calculating the pin-by-pin power distribution in an LWR core. Therefore the application of G-factors is eliminated.

9) Q. How does the CASMO-3G definition of the flux discontinuity factors ensure the bundle surface (flux) gradients are preserved in the nodal calculation?

A. Discontinuity factors are defined in CASMO-3G as the heterogeneous assembly surface flux (collapsed from the multigroup transport calculation) divided by the homogenized surface flux. The homogenized surface flux for each direction is computed by solving the one dimensional two group diffusion model of the assembly in which: 1) cross sections and diffusion coefficients are defined by flux-volume weighting with the COXY calculated fluxes 2) the COXY net surface currents are taken as boundary conditions, and 3) the flux is assumed to have a fourth order polynomial flux shape that is the same as that used in the SIMULATE-3 code. Since this flux shape is determined with the surface currents as boundary conditions, this assures that a SIMULATE-3 calculation corresponding to the CASMO-3G geometry will reproduce the CASMO-3G net currents, or flux gradients, on each surface.

10) Q. Since the CLOSEUP library only includes P_0 scattering, how is the gamma scattering anisotropy treated in the CASMO-3G gamma transport calculation?

A. The CLOSEUP library contains P_1 scattering cross sections, however only the P_0 cross sections are used by CASMO-3G to calculate the transport corrected cross sections by the formula:

$$\sigma_{t,r,n,g} = \sigma_{n,g}^0 - \sum_{g' \geq g} \sigma_{n,g-g'}^1$$

where σ^0 and σ^1 are the P_0 and P_1 scattering cross sections, respectively.

The gamma fluxes within an assembly are typically used to calculate the detector response function for the assembly. The flux distribution is flat and only sources which are close to the detector contribute significantly to the response. Therefore the gamma detector response is insensitive to the choice of the transport correction.

11) Q. Provide a description of the method used in CASMO-3G to calculate the baffle/reflector cross sections. Indicate the assumptions made in deriving the baffle cross sections and discuss their impact on predicted power distributions. How do these cross sections vary with fuel loading and core state variables? Are any ad-hoc adjustments or normalizations made to these cross sections? How is the baffle/reflector region treated in cold shutdown margin or cold critical calculations?

- A. CASMO-3G computes baffle/reflector cross sections by performing a detailed multigroup transport flux calculation in a one or two dimensional model containing one fuel assembly, the baffle, and the reflector. Pin cross sections for this calculation are generated using the same microgroup and macrogroup calculations as in a standard assembly calculation. The fuel assembly is used primarily to generate a flux spectrum in the baffle and reflector, and the few group reflector data is insensitive to the choice of fuel assembly. The baffle and reflector can consist of from one to three material regions.

The baffle/reflector data needed for few group core calculations is defined by the flux-volume weighting and collapsing of cross sections in the baffle and reflector regions. These cross sections alone, when used in a few group diffusion calculation, will not properly predict the core leakage. Therefore, CASMO-3G uses homogenization theory to define appropriate values of discontinuity factors for the baffle and reflector regions such that a few group diffusion solution will produce the same net current at the fuel/baffle interface as the multigroup transport solution. Subsequent use of these discontinuity factors and cross sections assures that few group diffusion solutions will properly predict leakage in a core calculation. No ad-hoc adjustments of the baffle/reflector cross sections are used in defining the CASMO-3G reflector data.

The SIMULATE-3P model uses the baffle/reflector cross section and Assembly Discontinuity Factor (ADF) data with a one node thick reflector, and an analytic boundary condition which assumes an infinite reflector. This provides essentially the same solution as when an infinite reflector is modelled.

The reflector cross sections for the power operation range are typically functionalized by TABLES-3 versus moderator density and boron concentration for a PWR and versus void fraction for a BWR. Therefore, cross sections for the reflector nodes in a SIMULATE-3P model are based on the actual reactor conditions. For cold conditions, an isothermal cross section library is generated along with appropriate reflector cross sections.

Upper and lower axial reflectors are treated in the same manner as the radial reflectors. The one dimensional axial model is represented by radially homogenizing the structural components, fuel rod plenums, and moderator above or below the fuel. Cross sections and ADFs are generated as a function of boron concentration and moderator density.

Within a typical range of fuel assembly design parameters, the spectral differences do not significantly affect the homogenization. A study was performed to demonstrate this. It analyzed the effect of using reflector cross section data developed with a fresh assembly for a typical low leakage reload core, where highly burnt fuel is located in the core periphery. Figure 11.1 presents a comparison of the power distributions calculated with a 'fresh' reflector and a

'burnt' reflector. The only difference in these models is the fuel spectrum used to homogenize the reflector cross sections and calculate the reflector ADFs. The 'fresh' reflector was calculated using a fresh 2.7 w/o U-235 assembly and the 'burnt' reflector was calculated using the same assembly depleted to 40 GWd/Mt. The maximum assembly relative power difference was .005, with an RMS difference of .002. Initial fuel enrichment could have been used in the same problem with similar results. This example demonstrates the insensitivity of the fuel model used to generate reflector cross section data on the global calculation.

12. Q. *When the fundamental mode solution is used to modify the infinite lattice results to account for leakage effects, the calculation is carried out in either diffusion theory or the B₁ approximation. For typical BWR and PWR lattices, what is the difference in the calculated lattice parameters obtained by these two methods and which method is recommended?*

A. The fundamental mode calculation provides a buckling (B²) that solves the equation:

$$(\Sigma - \Sigma^0)\phi + D B^2 \phi = 1/k T \phi$$

where:

Σ = the total cross section matrix

Σ^0 = the zeroth moment of the scattering matrix

ϕ = the flux vector

D = the diffusion coefficient

B² = the buckling

k = the system eigenvalue

T = the fission spectrum

The fundamental mode calculation can be performed in three modes:

- search for k_∞ with B² set equal to zero (normal eigenvalue calculation)
- calculate k_{effective} with a user input value for B² (used to for pin cell critical calculations), or
- search for B² so that k_{effective} equals 1. B² is then the equal to the material buckling B_m². This is used for assembly depletion and provides the spectrum for cross section collapsing.

In the diffusion theory approximation (or P₁ approximation), the diffusion coefficient is defined as:

$$D_0^{P1} = 1 / 3\Sigma_{tr,g}$$

For the B₁ approximation, the diffusion coefficient is approximately:

$$D_0^{B1} = 1 / 3\Sigma_{tr,g} \{1 + 4/15 (B/\Sigma_{tr,g})^2\}$$

The B_1 approximation results in a leakage term which is sensitive to the buckling. For the situation where k_∞ is unity, the two methods result in the same diffusion coefficients. For the situation where k_∞ is not unity, for example a fresh unshimmed assembly, the B_1 approximation provides incorrect values for the diffusion coefficient. This is illustrated in Table 12.1, which compares the fast diffusion coefficients calculated using the B_1 and P_1 approximations for a 3.1 w/o PWR assembly with 0 and 24 integral fuel burnable absorber B,C shims. The shims are a thermal absorber, hence would not be expected to significantly affect D_1 . However, the B_1 approximation results in a 7.3 percent change in D_1 , compared to a 0.8 percent change in D_1 for the P_1 approximation.

The change in the B_1 diffusion coefficients with geometric buckling creates a bias in cores which contain segregated regions of fuel of differing reactivities. Use of the B_1 fundamental mode approximation has shown an out-in power tilt compared to measured data for fresh cores which have the higher enriched fuel on the periphery, and an in-out power tilt for low leakage reload cores with the fresh fuel located inboard. The P_1 method is therefore recommended over the B_1 approximation because it results in better power distribution comparisons to measured data.

Table 8.1
DIXY G-factors for CE Assemblies

<u>Region</u>	<u>Percent Initial Relative Difference¹</u>	<u>G-factor Group 1</u>	<u>G-factor Group 2</u>	<u>Percent Final Relative Difference¹</u>
CE-0 Guide Tube	-14.29	.966228	1.18189	0.01
CE-0 Water Gap	-2.29	.996330	1.02988	0.03
CE-8 Guide Tube	-17.06	.969943	1.19873	0.00
CE-8 Shim	16.06	.980833	.75787	0.01
CE-8 Water Gap	-3.70	.997647	1.03122	0.04

¹ 100 X (Absorption Rate_{DIXY} - Absorption Rate_{COXY}) / Absorption Rate_{DIXY}

Table 8.2
DIXY G-factors for a GE High Energy Bundle

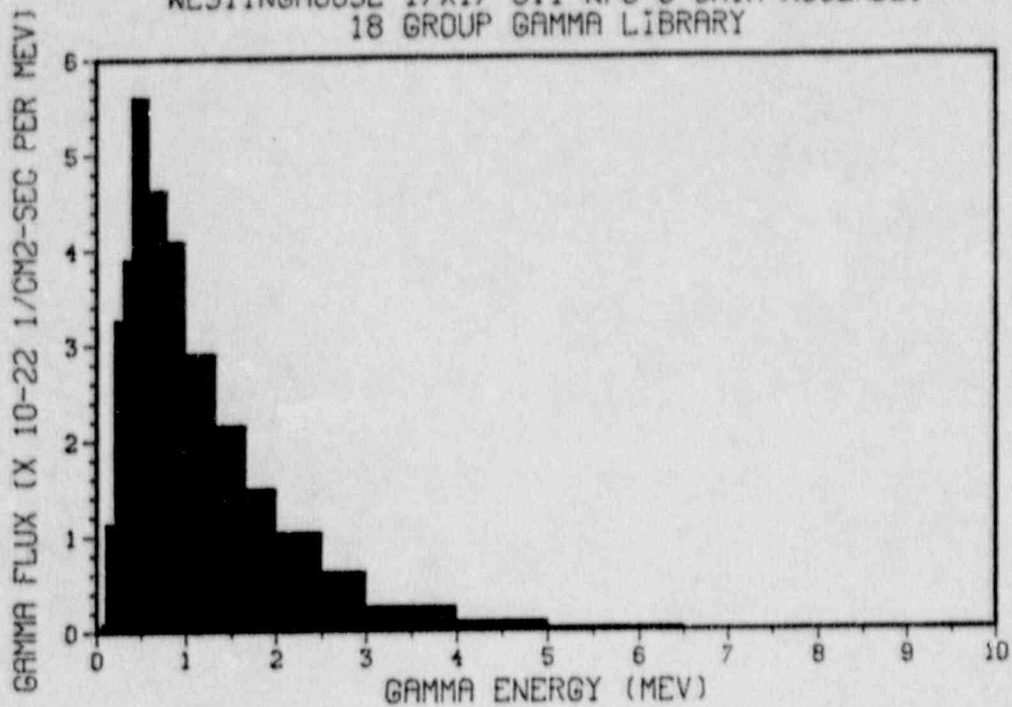
<u>Region</u>	<u>Percent Initial Relative Difference¹</u>	<u>G-factor Group 1</u>	<u>G-factor Group 2</u>	<u>Percent Final Relative Difference¹</u>
Gad Pin 1	18.00	1.00152	0.645233	-0.01
Gad Pin 2	19.15	0.993092	0.661948	-0.08
Gad Pin 3	17.40	1.01724	0.619952	-0.02
Water Rods	-20.57	0.991679	1.16298	-0.03
Box & Wide Water Gap	-12.86	0.951264	1.13987	-0.06
Box & Narrow Water Gap	-10.00	1.00949	1.07267	-0.04

¹ 100 X (Absorption Rate_{DIXY} - Absorption Rate_{CORY}) / Absorption Rate_{DIXY}

Table 12.1
Dependence of D_1
Versus Presence of a Thermal Absorber
Westinghouse PWR Assembly

<u>U-235</u> <u>W/O</u>	<u>Number of BP's</u>	<u>Diffusion Coefficient</u>	
		<u>D_1</u>	<u>D_2</u>
3.1	0	1.321	1.451
3.1	8	1.352	1.448
3.1	20	1.401	1.442
3.1	24	1.418	1.440

FIGURE 1.1
 GAMMA ENERGY SPECTRUM AT DETECTOR
 WESTINGHOUSE 17X17 3.1 W/O O SHIM ASSEMBLY
 18 GROUP GAMMA LIBRARY



10 GROUP GAMMA LIBRARY

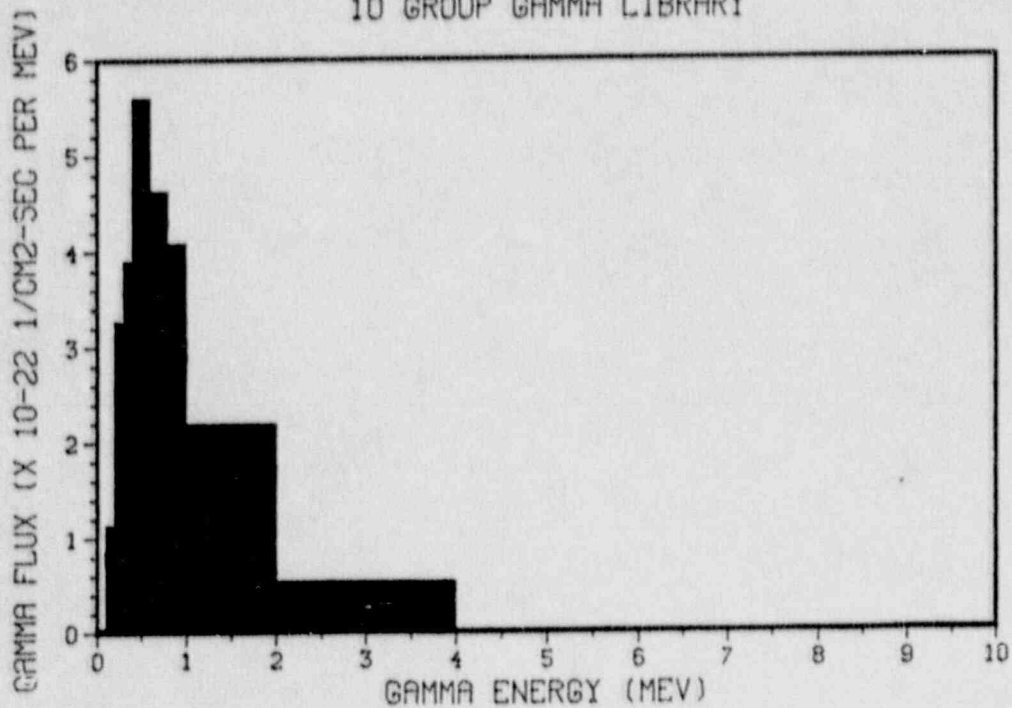


Figure 11.1
Core Power Distribution Comparison
Low Leakage PWR Reload Cycle
'Fresh' and 'Burnt' Reflector Cross Sections

	9	10	11	12	13	14	15	16	17
9	0.912	1.189	1.223	1.237	1.125	1.014	1.056	0.883	
	0.914	1.192	1.226	1.239	1.127	1.015	1.056	0.882	
	.002	.003	.003	.002	.002	.001	.000	-.001	
10	1.189	1.325	1.101	1.350	0.997	1.331	1.112	1.085	0.349
	1.192	1.327	1.103	1.353	0.998	1.332	1.112	1.084	0.348
	.003	.002	.002	.003	.001	.001	.000	-.001	-.001
11	1.223	1.108	1.005	1.220	1.309	1.151	1.099	1.071	0.306
	1.226	1.110	1.007	1.222	1.311	1.152	1.099	1.067	0.304
	.003	.002	.002	.002	.002	.001	.000	-.004	-.002
12	1.237	1.353	1.222	1.333	0.949	1.247	1.070	0.861	
	1.239	1.356	1.224	1.335	0.949	1.247	1.070	0.856	
	.002	.003	.002	.002	.000	.000	.000	-.005	
13	1.125	0.996	1.308	0.946	0.854	1.093	1.002	0.345	
	1.127	0.998	1.310	0.947	0.854	1.093	1.001	0.343	
	.002	.002	.002	.001	.000	.000	-.001	-.002	
14	1.014	1.329	1.148	1.241	1.086	0.989	0.397		
	1.015	1.330	1.149	1.241	1.086	0.988	0.394		
	.001	.001	.001	.000	.000	-.001	-.003		
15	1.056	1.111	1.095	1.064	0.992	0.383			
	1.056	1.111	1.095	1.063	0.991	0.381			
	.000	.000	.000	-.001	-.001	-.002			
16	0.883	1.082	1.067	0.855	0.342				
	0.882	1.081	1.064	0.851	0.340				
	-.001	-.001	-.003	-.004	-.002				
17		0.335	0.305						
		0.334	0.302						
		-.001	-.003						

0.335 'fresh' reflector assembly relative power
0.334 'burnt' reflector assembly relative power
-.001 difference = 'burnt' - 'fresh'